Catalysis Today 137 (2008) 453–459

Contents lists available at ScienceDirect

Catalysis Today

journal homepage: www.elsevier.com/locate/cattod

Steam reforming of ethanol over Ni/support catalysts for generation of hydrogen for fuel cell applications

Andrzej Denis, Wieslaw Grzegorczyk, Wojciech Gac, Andrzej Machocki *

University of Maria Curie-Sklodowska, Faculty of Chemistry, Department of Chemical Technology, 3 Maria Curie-Sklodowska Square, 20-031 Lublin, Poland

ARTICLE INFO

Article history:
Available online 2 May 2008

Keywords:
Hydrogen
Bio-ethanol
Steam reforming
Nickel catalyst
Catalyst support

ABSTRACT

The paper reports experimental results concerning the influence of the support nature (TiO_2, ZnO, Al_2O_3 and Al_2O_3–Fe_2O_3) of nickel catalysts on their activity, selectivity and coking phenomenon in the steam reforming of ethanol in the range of 570–870 K. The chemical transformations of ethanol occurring on the catalyst support make its chemical nature an important factor affecting the productivity and selectivity of the process. It was found that the most suitable supports in nickel catalysts designed for hydrogen generation in the steam reforming of ethanol are ZnO and TiO_2. Taking into consideration both the efficiency of hydrogen generation and the intensity of carbon deposition, the optimum temperature of the process of the steam reforming of ethanol is below 750 K. An improvement in the selectivity of hydrogen generation and diminishing of the formation of undesirable products may be obtained by promoting nickel catalysts with sodium.

1. Introduction

Hydrogen is expected to become an alternative fuel and a significant source of clean energy via fuel cell systems in the near-, medium- and long-term future. In a long-term perspective the generation of hydrogen should be environmentally friendly technology, in the broad sense of the term, and based on very effective processes. The most appropriate solution is thought to be solar energy utilization (via photo-electrolysis or direct photolytic water decomposition). Until much progress is made in this field, sources of hydrogen may be found in many various processes utilizing a variety of raw materials. For stationary big users or those within the range of the distribution network, hydrogen will probably be obtained from natural gas or from coal gasification. For some mobile users and, mainly for small stationary but scattered users having no access to hydrogen distribution network, a good solution seems to be the conversion of liquid fuels, such as alcohols or hydrocarbons, realized directly in the site of hydrogen use. That is why the necessary component of the system containing a fuel cell in such applications is a catalytic generator (reactor and reformer) for hydrogen generation from fossil or renewable resources [1].

From the environmental point of view the combination of hydrogen generation from bio-ethanol (a renewable resource, no additional carbon dioxide is released into the atmosphere) and the growing implementation of fuel cells (an advantageous power production technology with the high-energy efficiency) will bring benefits in the lowering of harmful emission and thus improving air quality. It could also increase energy security.

The generation of hydrogen from bio-ethanol may be carried out in the catalytic process in the presence of steam. The stoichiometry of the reaction of steam reforming implies a potential possibility of high efficiency of hydrogen production: one mole of ethanol may yield six moles of hydrogen ($C_2H_5OH + 3H_2O = 6H_2 + 2CO_2$); putting it in different terms, 50 cm^3 of 95% ethanol should be enough to generate almost 110 l of hydrogen. However, the final hydrogen productivity will depend on the intensity and the state of the equilibrium of the water gas shift reaction ($H_2O + CO = H_2 + CO_2$), as well as successful inhibition of non-selective transformations of ethanol to acetaldehyde, ethylene, methane and other by-products which may be formed in successive side reactions. A balanced, thermodynamic productivity of hydrogen, taking into account the participation of side reactions, is estimated to be about 5.5 mol of H_2 formed from 1 mol of ethanol [2].

So far there are no commercial catalysts available for the ethanol steam reforming process. There has been no need for them since we only witness intense preparations for an expansion of hydrogen power industry. Research papers published so far do not report clear preferences concerning the chemical composition of the most advantageous catalyst of the ethanol steam reforming. As an active phase researchers consider first of all: noble metals, nickel and cobalt [3–9]. From the formal point of view, the generation of hydrogen through the steam reforming of ethanol

* Corresponding author. Tel.: +48 815375514; fax: +48 815375565.
E-mail address: machocki@hermes.umcs.lublin.pl (A. Machocki).

0920-5861/$ – see front matter © 2008 Elsevier B.V. All rights reserved.
doi:10.1016/j.cattod.2008.03.006

seems to be a process analogous to the steam reforming of natural gas and it would seem that nickel catalysts employed in the latter process met also the requirements of ethanol steam reforming. However, the significant differences in the course of the steam reforming of ethanol and that of methane are caused by more complicated structure of a molecule of ethanol due to the presence of a C–C bond and oxygen atom. It induces more complex pathways of its transformations and the number of potential by-products formed from ethanol is therefore greater than those formed from methane. The most effective metal considered as the active phase of catalyst designed for the steam reforming of ethanol is rhodium because it shows the greatest activity towards C–C cleavage [3,4,6,9–11]. However, the high price of rhodium leans to seeking after a less expensive catalyst. Some interesting attempts with the use of nickel-based catalysts are reported in Refs. [3,5–9,12–43]. This study also falls into this trend.

The chemical transformation of ethanol occurring on the catalyst support and different interactions of nickel with the support make its chemical nature an important factor affecting the productivity and selectivity of the process [3–9,17,19,21,26,32,38]. The participation of various thermodynamically possible courses of the reaction is determined not only by the character of the active phase but, to a large extent, also by the character of the support. The reaction of ethanol dehydration produces ethylene. Such a course of ethanol transformation is facilitated by oxides with acidic surface. Therefore it would seems advantageous to employ supports promoted by alkali metals [3,4,6–9,30,31,36,42], modified by additions of other oxides [3,5–7,9,13,15,16,18,27,37], or pure oxides of alkaline or weakly alkaline nature. Besides, it is well known that the active phase of metallic nickel is very susceptible to the formation of carbonaceous deposit in contacts with hydrocarbons and their derivatives, thus causing catalyst deactivation. The latter phenomena may constitute a very important problem demanding a solution in the cases of catalysts of the steam reforming of ethanol.

The far-reaching aim of our studies was to develop a catalyst for the hydrogen generation in the steam reforming of ethanol. The present paper reports experimental results concerning the influence of the support nature (Al_2O_3, TiO_2, ZnO and Al_2O_3–Fe_2O_3) of nickel catalysts on their activity, selectivity and intensity of coking in the steam reforming of ethanol. We expected that the Al_2O_3–Fe_2O_3 support, due to the presence of Fe_2O_3, as well as the ZnO support, will create a positive effect on the water gas shift reaction. The effect of the presence of a sodium promoter on the properties of catalysts Ni/Al_2O_3 and Ni/ZnO was also examined.

2. Experimental

The supported nickel catalysts were prepared by the method of incipient wetness impregnation of TiO_2 (Degussa P25, mainly composed of the anataze phase, 50 m^2/g), ZnO (INS Pulawy, Poland, 48 m^2/g), Al_2O_3 (Peshiney, prior to its use original alumina was sintered in air at 500 °C for 20 h, composed mainly of the γ-Al_2O_3 phase, 250 m^2/g) or Al_2O_3–Fe_2O_3 (27.1 wt.% of Fe_2O_3, 50 m^2/g) using nickel nitrate as a metal precursor. Al_2O_3–Fe_2O_3 support was obtained by precipitation of ferrous ions on the alumina powder suspended in an aqueous solution of ferrous nitrate by sodium carbonate Na_2CO_3 as precipitating agent, washing, drying at 380 K and 6-h calcinations at 870 K. The operations of support impregnation with nickel solution were carried out twice, introducing at each step a half of the required total nickel loading. The catalysts were signed with the Ni/Ti, Ni/Zn, Ni/Al and Ni/Al–Fe symbols. The catalyst precursors were dried at 380 K, calcined at 670 K for 6 h and finally, prior to their use, all catalysts were reduced with hydrogen at 670 K for 1 h. The nickel loading in the catalysts was equal to 10 wt.%. The calcined Ni/Zn and Ni/Al catalysts were additionally promoted with 1 wt.% (nominal, without of analytical control of the real contents) of sodium by their additional impregnation with the Na_2CO_3 solution according to the same procedure. Non-negligible amounts of sodium can be present in some of the supports themselves (e.g. according to its producer, Al_2O_3 contains <0.6 wt.% of Na). However, our intention was to introduce greater amounts of sodium on the catalyst surface, not only on the support but also on the nickel phase. Since nickel in the calcined catalysts was in the oxide form we did not expect that those additional impregnations could significantly decrease of its content in the final catalysts. Therefore, the contents of nickel in the Ni/Zn + Na and Ni/Al + Na catalysts were not checked after sodium introduction. The data regarding characterization of catalysts are presented in Table 1.

The bulk contents of nickel and iron in catalysts were determined by the X-ray fluorescence spectroscopy technique, by means of an energy-dispersive XRF spectrometer (Canberra 1510) equipped with the liquid nitrogen-cooled Si(Li) detector. The AXIL software package was used for spectral deconvolution and for the calculation of the nickel component (and iron in the case of the Ni/Al–Fe catalyst) contents.

The porosity and the total BET surface area of the supports and catalysts were measured by the low-temperature (77 K) nitrogen adsorption in the ASAP 2405N v1.0 analyser (Micromeritics), assuming that one nitrogen molecule occupies the area of 0.162 nm^2. The average pore diameters and the volume of pores were calculated from the desorption data using the Barret–Joyner–Halenda (BJH) method [44].

Hydrogen chemisorption at 308 K was measured in the Autosorb-1-C analyser (Quantachrome). Prior to the measurements, catalysts were reduced *in situ* with hydrogen at 670 K for 1 h in a sample cell of the Autosorb analyser. Then, they were cooled down to 570 K under flowing H_2, degassed at that temperature under vacuum of 5×10^{-7} Pa and, after cooling to 308 K, the hydrogen chemisorption was measured. The uptake of hydrogen due to its chemisorption was determined by extrapolating the straight-line portion of the isotherm (up to the equilibrium pressure of 13.3 kPa) to zero pressure. The surface area of the nickel active phase was calculated on the basis of the total hydrogen chemisorption

Table 1
Catalyst characterization results

Catalyst	BET surface area (m^2/g_{cat})	Volume of pores (cm^3/g_{cat})	Average pore diameter (nm)	Nickel surface area (m^2/g_{cat})	Mean size of nickel crystallites (nm)	Reduction degree (%)
Ni/Al	236.3	0.3461	4.82	2.1	>10[a]	3.6
Ni/Ti	42.6	0.2999	22.68	2.6	14.0	29.6
Ni/Zn	6.3	0.0254	13.33	2.2	24.0	22.3
Ni/Al–Fe	6.4	0.0208	15.04	2.7	16.3	–[b]
Ni/Al–Na	226.1	0.3366	4.64	–	>10[a]	14.0
Ni/Zn–Na	2.1	0.0118	24.95	–	65.0	–[b]

[a] Since very small intensity of the strongest X-ray line (1 1 1) of nickel the determination of mean size of nickel crystallites was saddled with a large error.
[b] Because of partial reduction of the support oxides the formal reduction degree at 670 K was higher than 100%.

assuming that one hydrogen atom is adsorbed on the area occupied by one surface nickel atom (the stoichiometry of the chemisorption is Ni:H = 1:1) and that the surface area occupied by one atom of hydrogen equals to 0.065 nm^2.

X-ray powder diffraction patterns of catalysts were collected with an upgraded Zeiss HZG-4 diffractometer using Mn-filtered Cu Kα radiation. The *ex situ* reduced (with hydrogen at 670 K for 1 h) samples were transferred in helium filled sample vials into the XRD system after their quick cooling in hydrogen and careful passivation at room temperature with a stream of nitrogen containing very small amount (<0.1%) of oxygen. The samples were scanned by a step-by-step technique, at 2θ intervals of 0.05° and recording time of 10 s for each step. The measured patterns were compared with the joint committee on powder diffraction standards (JCPDS) database for phase identification. The average size of the nickel crystallites was estimated from X-ray diffraction line broadening of the peak corresponding to the (1 1 1) crystal plane, using Scherrer equation.

The temperature-programmed reduction of the catalysts was carried out in the apparatus AMI-1 (Altamira Instruments Inc.) using 0.05 g of catalyst (0.1–0.2 mm) placed in a flow quartz reactor with an internal diameter 7 mm. A 6% H_2–Ar mixture was used as carrier gas at a flow rate of 30 cm^3/min.; the linear temperature increase was 10 K/min. Water vapour formed during reduction was removed in a cold trap (immersed in liquid nitrogen–methanol slush, at 175 K) placed before the thermal conductivity detector (TCD). The TCD signal was calibrated by injecting 55 μl of argon to the carrier gas. The reduction degree of catalysts at 670 K was estimated from the TPR results by assuming that hydrogen was consumed only for nickel oxide reduction to metallic nickel. Therefore, they are not true when reduction of support oxides occurred.

The steam reforming of ethanol was carried out under atmospheric pressure in a fixed-bed continuous-flow quartz reactor over catalysts (0.1 g, grain size of 0.5–0.7 mm) reduced *in situ* with hydrogen at 670 K for 1 h, prior to the reaction. The catalyst was diluted (at the weight ratio of 1:10) with 0.5–0.7 mm grains of quartz in order to ensure the constant temperature in the catalytic layer. In a preliminary experiment it was found that the conversion of ethanol over quartz starts, in a small extent, at higher temperatures (>970 K) than those at which the steam reforming of ethanol in the presence of catalysts was investigated. The aqueous solution of ethanol (with a molar EtOH/water ratio equalled to 1/4) was supplied by a peristaltic pump (Masterflex LS with 7013-20 head) to a liquid preheater/evaporator (423 K) and the reactant vapours without diluting with any inert gas were fed to the reactor at the flow rate of 0.2697 mol/h. The reaction temperature, measured in the centre of the catalyst + quartz bed, was changed from 573 to 873 K. The temperature was increased step-by-step and analyses of the reaction products were conducted several times during about 2 h of the reaction at each of the temperatures. The analysis after 0.5 h was selected to present the temperature dependences of the initial reactant conversions and selectivities.

The analysis of the reaction mixture and the reaction products (all in a gas phase) were carried out on-line by means of two gas chromatographs. One of them, Varian CP-3800 was equipped with two capillary columns, the first one contained a porous polymer Poropak Q (for all organics, carbon dioxide and water vapour) and the second of them—an activated molecular sieve 5A (for methane and carbon monoxide analysis). Helium was used as a carrier gas and a TCD detector was employed. The hydrogen concentration was analysed by the second gas chromatograph, Chromatron GCHF 18.3, using a column packed with an activated charcoal, nitrogen as a carrier gas and a TCD detector. The sensitivity of the detectors to the analysed compounds (response factors) was determined, before and after each catalytic test, by their calibration against external standards of single compounds or their certified (Praxair) mixtures composed of carbon oxides and hydrocarbons in helium. The concentrations of the external standards were comparable with those of analysed products. The reproducibility of the analysis of the components of the certified mixtures was about ±2%.

The total conversion of ethanol X_{EtOH}, conversion of water X_{H_2O} and conversions of ethanol into particular carbon-containing products, X_{CP}, were calculated on the basis of their concentrations before and after the reaction, with a correction introduced for the change in a gas volume during the reaction, from equations:

$$X_{EtOH} = \frac{c^{in}_{EtOH} - c^{out}_{EtOH}K}{c^{in}_{EtOH}} \times 100, \qquad X_{H_2O} = \frac{c^{in}_{H_2O} - c^{out}_{H_2O}K}{c^{in}_{H_2O}} \times 100,$$

$$X_{CP} = \frac{c^{out}_{CP}K}{(n/2)c^{in}_{EtOH}} \times 100(\%)$$

where c^{in}_{EtOH} and $c^{in}_{H_2O}$ are the molar concentrations of ethanol and water in the reaction mixture, mol%; c^{out}_{EtOH} and $c^{out}_{H_2O}$ are the molar concentrations of ethanol and water in the post-reaction mixture, mol%; c^{out}_{CP} is the molar concentration of carbon-containing products in the post-reaction mixture, mol%; n is the number of carbon atoms in the carbon-containing molecule of the reaction product; K is the volume contraction factor ($K = c^{in}_C / c^{out}_C$ where: c^{in}_C and c^{out}_C are the molar concentrations of carbon in ethanol fed to the reaction and in all carbon-containing compounds which were present in post-reaction gases, respectively).

The selectivity of ethanol conversion into individual carbon-containing products was expressed as $(X_{CP}/X_{EtOH}) \times 100$. The carbon mass balances, based on the carbon selectivities at each of the reaction temperatures, were close to 100 ± 3%.

The hydrogen and oxygen balances were not recorded. The selectivity of hydrogen formation was determined from the equation:

$$H_2\text{-selectivity} = \frac{c^{out}_{H_2}}{c^{out}_{H_2} + 2c^{out}_{CH_4} + 2c^{out}_{C_2H_4} + 2c^{out}_{CH_3CHO} + 3c^{out}_{C_2H_6}} \times 100(\%)$$

where c^{out} is the molar concentrations of the hydrogen-containing reaction products, mol%.

The studies of the catalyst coking under the steam reforming of ethanol conditions were performed by the gravimetric method using the conventional microbalance TG121 System (Cahn) under dynamic conditions in a quartz reactor with a continuous flow of ethanol–water vapours. The sensitivity of the balance was 0.1 μg. Those experiments simulated the activity measurement tests but the catalyst sample was placed on a small quartz plate. The *in situ* reduced (with hydrogen at 670 K for 1 h) catalyst samples (0.01 g, 0.1–0.2 mm) were cooled down to 470 K in a flow of hydrogen. Then the reactor was flushed with nitrogen and the catalyst samples were heated up to the 870 K in the stream of the ethanol and water vapour mixture ($EtOH/H_2O$ = 1/4, 0.2697 mol/h, without diluting with any inert gas) with the heating rate of 2 K/min. The reactant mixture was introduced to the microbalance reactor in the same way as during the activity measurement tests.

3. Results and discussion

3.1. Catalyst characterization

The total surface area, volume of pores and their average diameters as well as nickel surface area and mean size of nickel crystallites in reduced catalysts are presented in Table 1. The reduction degrees of nickel are also included. The total surface areas of all catalysts are somewhat lower than those of the initial supports, indicating blockage of pores by the nickel phase. The

differences in textural properties of catalysts are evident, particularly the total surface area and the porosity of Al_2O_3 supported catalysts are much higher than those of the remaining catalysts. In all catalysts the metallic phase of nickel after reduction at 670 K possessed a similar surface area, from 2.1 to 2.7 m^2/g_{cat}.

The XRD patterns indicated the presence of the support oxides, metallic nickel and unreduced nickel oxide. The XRD analysis of the modified Al_2O_3–Fe_2O_3 support and calcined Ni/Al–Fe catalyst showed that the ferrous phase remained in the form of a high-dispersed mixture of hematite, with a small amounts of magnetite (Fe_2O_3 and Fe_3O_4). The XRD patterns did not indicate the presence of other phases, including those of the type of spinels or hydrotalkite. After the catalyst reduction, the metallic phase of nickel and iron (traces), as well as very weak broadened diffraction lines of the Fe_3O_4 phase were identified. In the case of reduced Ni/Zn + Na catalyst the 0.5° shift of the Ni reflection was observed, suggesting [18] a partial dissolution of Zn^0 in Ni^0 and the NiZn alloy presence.

The mean size of nickel crystallites in most of reduced catalysts was in the range of 14–24 nm (Table 1). The NiZn alloy average diameter in the Ni/Zn + Na catalyst was much higher, i.e. 65 nm. Since the diffraction reflections of nickel in the Ni/Al and Ni/Al + Na catalysts were very low, the precise determination of the crystallite sizes was saddled with large inaccuracies. However, the nickel crystallites in those catalysts were greater than 10 nm. Generally, the crystallite sizes of nickel in all catalysts were in the range where the influence of dispersion on the activity of catalysts prepared by the impregnation method was not significant [24].

The TPR results (Fig. 1) confirmed different reducibility of the catalysts. The low-temperature peak of hydrogen consumption is attributed to the reduction of bulk nickel oxide with weak interactions with the support. In the Ni/Al catalyst those interactions are very strong, the reducibility of nickel oxide in the range of lower temperatures is very hard. In the case of the Ni/Al–Fe catalyst the low-temperature peak composes of two clearly marked peaks, which indicate co-reduction of nickel and iron oxides. The hydrogen consumption peaks at higher temperatures are associated with the reduction of nickel ions strongly interacted

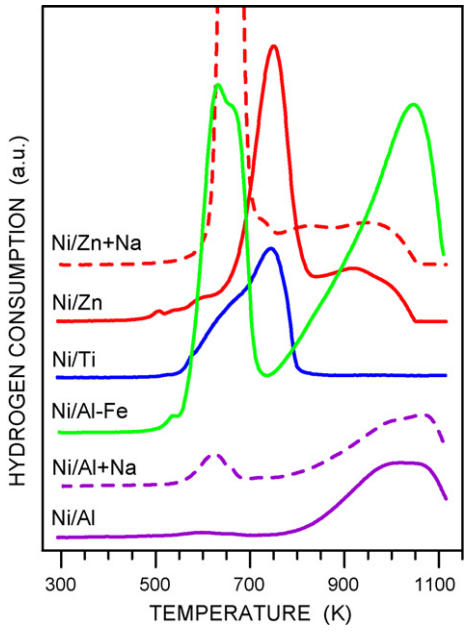

Fig. 1. H_2-TPR profiles of nickel catalyst with various supports and promoted with sodium.

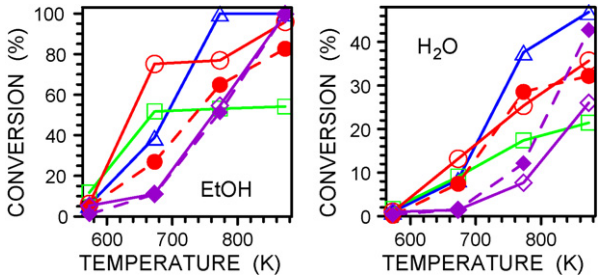

Fig. 2. Effect of nickel catalyst support and sodium promoter on the conversion of ethanol and water in the steam reforming of ethanol: (◇) Ni/Al; (Δ) Ni/Ti; (○) Ni/Zn; (□) Ni/Al–Fe; (◆) Ni/Al + Na; (●) Ni/Zn + Na.

with the support oxides. In the case of the Ni/Al–Fe catalyst the large high-temperature peak may be attributed to the co-reduction of nickel ions and ferrous phase of the support. In the case of Ni/Zn and Ni/Zn + Na catalysts the support underwent reduction in some extent. Such possibility was also shown in Refs. [18,26]. It is noticeable that the presence of sodium facilitates reduction of nickel oxide in both promoted catalysts, Ni/Al + Na and Ni/Zn + Na. In the later catalyst the ZnO reduction was also facilitated and the formation of the NiZn alloy even at 670 K we have found in the XRD measurements.

The nickel oxide reduction degrees at 670 K, determined from the TPR results, were rather low (Table 1). However, we expect that they will change in the reaction of the steam reforming of ethanol as it was shown in the reports [3,18]. Nickel oxide should undergo reduction in an extent depending on the reaction conditions, i.e. on the temperature and on the gas phase composition (i.e. also on reagent conversions and reaction selectivity). Similar reduction of a cobalt oxide phase was reported in [3,6]. The pre-reduction of our catalysts at 670 K was applied in order to accelerate changes in nickel–nickel oxide proportions during the steam reforming of ethanol, especially at low temperatures.

3.2. Activity and selectivity of unpromoted nickel catalysts in the ethanol steam reforming

At 570 K the activity of all examined catalysts is very small and ethanol conversion reaches only about 5% (Fig. 2). The total conversion of ethanol on the Ni/Ti catalyst was obtained at 770 K. With nickel supported on modified alumina, i.e. on the Ni/Al–Fe catalyst, at the temperature of 870 K the obtained ethanol conversion was only 54%, whereas on another sodium-free catalysts at the same temperature ethanol conversions exceeded 95%, and in most cases the conversions were equal to 100%. The degree of water conversion (Fig. 2) is smaller than that of ethanol. It is caused, on one hand, by the excess of the amount of water vapour in the reaction mixture in relation to the stoichiometry of the reaction $C_2H_5OH + 3H_2O = 6H_2 + 2CO_2$, and, on the other hand, by non-selective ethanol transformations occurring without the participation of water (Fig. 3). The catalytic activity of nickel in the range of higher temperatures, 770–870 K, decreases in the order: Ni/Ti > Ni/Zn > Ni/Al ≫ Ni/Al–Fe.

In the range of lower temperatures the highest activity was shown by the Ni/Zn catalyst, which – at the temperature of 670 K – enabled conversions over 75% of ethanol and 13% of water (Fig. 2). The least advantageous nickel support for the reaction at low temperatures was Al_2O_3. Over the Ni/Al sample, at the same temperature, only 11% of ethanol conversion and merely the 1.5% water conversion were obtained. The low activity of the Ni/Al catalyst at 670 K is probably associated with a presence of small amounts of metallic nickel—it is seen in Fig. 1 that the reduction of nickel ions in Ni/Al catalyst was very difficult. At that temperature

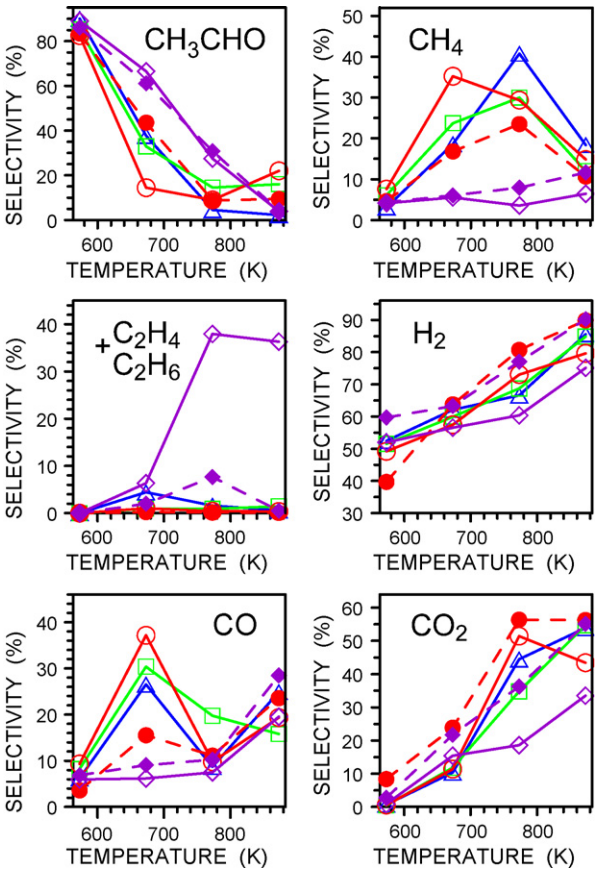

Fig. 3. Effect of nickel catalyst support and sodium promoter on selectivity of the steam reforming of ethanol: (◇) Ni/Al; (Δ) Ni/Ti; (○) Ni/Zn; (□) Ni/Al–Fe; (◆) Ni/Al + Na; (●) Ni/Zn + Na.

among the reaction products acetaldehyde dominated (Fig. 3). The dehydrogenation of ethanol to acetaldehyde is a main direction of the ethanol transformation almost on all catalysts—it is a first step in the reforming of the ethanol process. An exception is the Ni/Zn catalyst, over which, at 670 K, the dominant by-product is methane and carbon monoxide (Fig. 3). Under such conditions the activity of this catalyst is high enough (Fig. 2) to ensure the high rate of one of subsequent stages of acetaldehyde transformations, i.e. its decomposition into CH_4 and CO on the surface of nickel.

The selectivity of the whole process of the conversion of ethanol to methane formed on three samples of catalysts (apart from the Ni/Al) passes through a maximum along with rising temperatures, which is in the agreement with the selectivity of the carbon monoxide formation (Fig. 3). The highest selectivity towards the methane formation and its productivity characterize catalysts of high activity, i.e. Ni/Zn and Ni/Ti. The formation of large amounts of methane as a transition product of the ethanol conversion is disadvantageous so far because its subsequent reaction with water will require high temperatures, typical of the process of the steam reforming of natural gas.

A strong influence of the support is also observed in the activity of nickel in reactions of the formation of ethylene and ethane. In the temperature range of up to 670 K on all catalysts the process takes place with a very similar selectivity and productivity of the formation of ethylene and ethane (up to 9×10^{-4} mol/(h g_{cat})). The strong influence of the Al_2O_3 support on the selectivity towards ethylene is revealed only above 670 K (Fig. 3). At 870 K the productivity of ethylene on the Ni/Al catalyst is about 100-times higher than that observed on other catalysts and under the used experimental conditions it was 1.9×10^{-2} mol C_2H_4/(h $g_{cat.}$). It should be emphasized that for most catalysts the selectivity to ethane practically remains on a constant, low level: from 0 at 570 K to 1% at 870 K. Exceptionally, more ethane than ethylene is formed on the Ni/Ti catalyst at 670–770 K.

At temperatures up to 770 K (with a maximum at 670 K) over Ni/Ti, Ni/Zn and Ni/Al–Fe catalysts the dominant component of oxidation is carbon monoxide (Fig. 3). The high selectivity towards carbon monoxide was obtained over catalysts composed of oxides (ZnO and Al_2O_3–Fe_2O_3) that are crucial components of water gas shift reaction catalysts. The lowest selectivity to CO was obtained for the Ni/Al catalyst. Above 770 K the selectivity of the formation of carbon monoxide raises again. Carbon monoxide is one of the undesirable products of the process of reforming because, even in the presence of trace amounts it poisons the platinum anodes of low-temperature fuel cells, e.g. solid polymer electrolyte fuel cells, proton-exchange membrane electrolyte fuel cells (SPEFCs, PEMFCs), which are regarded to be most suitable for the application in small stationary power plants. One may hope that in the near future new electrode materials, tolerating the presence of carbon monoxide [45], will be developed which can solve the problem of the purity of hydrogen-rich gases generated from hydrocarbons or alcohols, also including ethanol.

The course of the reaction of the ethanol reforming in the most desirable direction – the formation of H_2 and CO_2 – is ensured by higher temperatures (Fig. 3). The selectivity of the formation of carbon dioxide, similar over all catalysts at 570–670 K, becomes clearly differentiated at higher temperatures. A similar situation is observed in the case of the hydrogen selectivity. At 770 K the most advantageous in this respect are Ni/Zn and Ni/Ti catalysts, the least advantageous is the Ni/Al system.

On the basis of both ethanol conversions and hydrogen selectivities one may get the following order of hydrogen productivity in the steam reforming of ethanol: Ni/Zn ≈ Ni/Ti > Ni/Al–Fe > Ni/Al (Fig. 4). Taking into account hydrogen productivity the optimum temperatures of this process are in the range of 770–870 K. In this temperature range one obtains the highest yield of hydrogen (expressed as moles of H_2 formed from 1 mol of reacted ethanol) and its highest productivity.

All reactant conversions and selectivities of the steam reforming of ethanol described above reflect the initial properties of catalysts. However, the activities and selectivities changed not only with the temperature but also during the reaction time. The variations of the conversions of ethanol and water over one of the most active catalyst, Ni/Zn, at each reaction temperature are shown in Fig. 5. The highest and the quickest changes in reactant conversions (and selectivities—not shown here) were observed at the temperatures of 773 K and higher. At lower temperatures of the reaction, i.e. at 573 and 673 K, the activities of all catalysts were more stable. The instability of the effects of the steam reforming of ethanol may be caused by sintering of the nickel phase and/or its

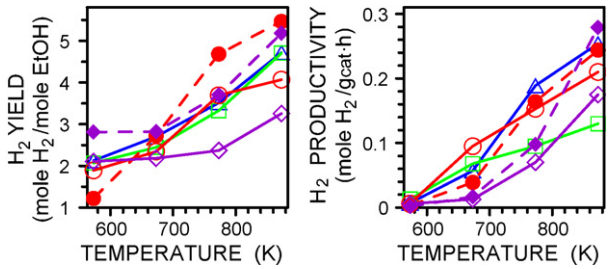

Fig. 4. Effect of nickel catalyst support and sodium promoter on the yield and productivity of hydrogen formation in the steam reforming of ethanol: (◇) Ni/Al; (Δ) Ni/Ti; (○) Ni/Zn; (□) Ni/Al–Fe; (◆) Ni/Al + Na; (●) Ni/Zn + Na.

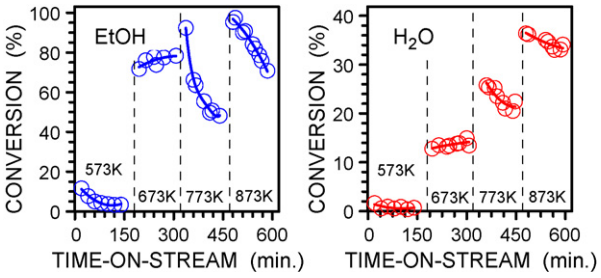

Fig. 5. Activity of the Ni/Zn catalyst vs. reaction time at various temperatures of the steam reforming of ethanol.

support as well as by a carbonaceous deposit formed on the surface of catalysts. In our studies, when the temperatures of the reaction were not very high the more significant reason of the catalysts deactivation seems their coking. The formation of carbonaceous deposit on nickel catalysts in the steam reforming of ethanol was reported in Refs. [3–7,9,12,15–17,19,24,28,30,31,35].

3.3. Coking of unpromoted nickel catalysts in the ethanol steam reforming

The ultimate usefulness of nickel catalysts for hydrogen generation in the process of the ethanol reforming depends on the complex of all stages of the process, including the participation of reactions leading to the appearance of very undesirable by-product, i.e. the carbonaceous deposit on the catalyst, that is one of the most significant causes of deactivation of catalysts.

Fig. 6 presents courses of catalyst coking in the atmosphere of the ethanol–water vapour reaction mixture. The significant changes in the weight of the catalysts, caused by the carbonaceous deposit formation, began at the temperature of 670 K in the case of the Ni/Zn catalyst and in the range of 720–740 K for another catalysts. It should be noticed that the convergence between the temperatures at which fast deactivation of catalysts were observed (Fig. 5) and those of the beginning of the significant coking of catalysts (Fig. 6).

The highest susceptibility to coking is shown by catalysts of the highest catalytic activity. It may results to some extent from their smaller porosity. In the conventional microbalance used in our experiments the influence of reactants/products diffusion to/from the catalyst grains and in its pores may govern the course of catalytic reaction. However, except of Ni/Al and Ni/Al + Na catalysts, the differences in the pore average diameters in the remaining catalysts were not very significant. Therefore, the observed coking effects can be related to the chemical nature of the catalyst oxide supports.

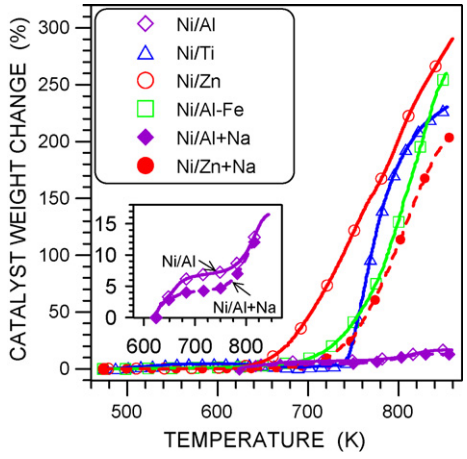

Fig. 6. Coking of supported nickel catalysts in the steam reforming of ethanol (symbols are used only for curves differentiation, they are not experimental points).

A proper selection of the support nature and its modification may therefore ensure the elimination of the reactions leading to the carbonaceous deposit. Taking into account both the coking intensities and the deactivation of catalysts, it may be recommended that the process of the steam reforming of ethanol over nickel catalysts should be carried out below 770 K rather than at higher temperatures. The water concentration in the reaction mixture should be also higher in order to restrict catalyst coking in the higher extent.

3.4. Performance of sodium promoted nickel catalysts in the ethanol steam reforming

In order to diminish the participation of undesirable reactions the Ni/Zn and Ni/Al catalysts were promoted with additional amounts of sodium. The Ni/Zn catalyst showed too high selectivity to carbon monoxide, while the Ni/Al catalyst—too large participation of the reaction of ethanol dehydration and ethylene formation. Both catalysts also underwent the phenomenon of coking, what is hard to ignore. At the temperature of 870 K, over the Ni/Zn + Na catalyst the methane formation was decreased from over 50 relative percent at the temperature of 670 K to 30 relative percent in comparison to that obtained for unpromoted Ni/Zn (Fig. 3). At the same time the catalyst's resistance to coking was increased, though still to an unsatisfactory extent. The rate of carbon deposition on the sodium promoted catalyst is by about 1/3 lower than that on the sodium-free catalyst (Fig. 6). On the other hand, the promotion of the Ni/Zn catalyst with sodium did not influence the selectivity to carbon monoxide at temperatures of 770 K and higher, yet it was still very advantageous in this respect at 670 K (Fig. 3).

The introduction of sodium to the Ni/Al catalyst caused only slight changes in the selectivity of methane formation. It was without any effect at low reaction temperatures, and above 770 K it caused a small increase in the formation of this product (Fig. 3). However, the presence of sodium very strongly inhibited the reaction of ethanol dehydration over aluminum oxide. Over the Ni/Al + Na catalyst the selectivity to ethylene dropped to the level similar to that obtained on other catalysts (Fig. 3). The essential benefit of the introduction of sodium into the Ni/Al catalyst (as well as into Ni/Zn) was also the increase of the carbon dioxide selectivity (Fig. 3). It should be stressed that at the same time sodium promoter did not change significantly the Ni/Al catalyst resistance to coking. However, the amounts of carbon formed on Ni/Al + Na at lower temperatures were smaller (Fig. 6). The presence of sodium promoter caused diminishing of the conversion of ethanol in the range of low temperatures (Fig. 2). Taking into account the productivity of hydrogen the positive effect of sodium promoting on the steam reforming of ethanol is confirmed only in the case of the Ni/Al catalyst (Fig. 4).

4. Conclusions

The general conclusion from the presented studies is that the most suitable supports in nickel catalysts designed for the steam reforming of bio-ethanol are ZnO and TiO_2. The oxide ferrous used for modification of alumina support had the disadvantageous influence on the activity of nickel. Taking into consideration both the efficiency of hydrogen generation and the intensity of carbon deposition, the optimum temperature of the process of the steam reforming of ethanol is below about 750 K. The significant excess of the amount of water (the H_2O/EtOH higher than 4/1) in the reaction mixture should be also recommended to restrict catalyst coking.

The nickel active phase and its support should be promoted or modified, thus diminishing the participation of undesirable reactions occurring on the surface of catalysts. An improvement of the selectivity of the process to hydrogen generation and diminishing of the formation of undesirable products (especially of hydrocarbons, including ethylene, and carbonaceous deposit) may be obtained by promoting nickel catalysts with sodium.

References

[1] A. Qi, B. Peppley, K. Karan, Fuel Process. Technol. 88 (2007) 3.
[2] K. Vasudeva, N. Mitra, P. Umasankar, S.C. Dhingra, Int. J. Hydrogen Energ. 21 (1996) 13.
[3] V. Subramani, Ch. Song, Catalysis 20 (2007) 65 (and references cited therein).
[4] M. Ni, D.Y.C. Leung, M.K.H. Leung, Int. J. Hydrogen Energ. 32 (2007) 3238 (and references cited therein).
[5] F. Frusteri, S. Freni, J. Power Sources 173 (2007) 200 (and references cited therein).
[6] P.R. Piscina, N. Homs, in: S. Minteer (Ed.), Alcoholic Fuels, Taylor & Francis, Boca Raton, 2006 , pp. 233–248 (and references cited therein).
[7] A. Machocki, Przem. Chem. 85 (2006) 1045 (and references cited therein).
[8] P.K. Cheekatamarla, C.M. Finnerty, J. Power Sources 160 (2006) 490 (and references cited therein).
[9] P.D. Vaidya, A.E. Rodrigues, Chem. Eng. J. 117 (2006) 39 (and references cited therein).
[10] D.K. Liguras, D.I. Kondarides, X.E. Verykios, Appl. Catal. B 43 (2003) 345.
[11] J.P. Breen, R. Burch, H.M. Coleman, Appl. Catal. B 39 (2002) 65.
[12] A.L. Alberton, M.M.V.M. Souza, M. Schmal, Catal. Today 123 (2007) 257.
[13] P. Biswas, D. Kunzuru, Int. J. Hydrogen Energ. 32 (2007) 969.
[14] M. Benito, R. Padilla, L. Rodriguez, J.L. Sanz, L. Daza, J. Power Sources 169 (2007) 167.
[15] J.W.C. Liberatori, R.U. Ribeiro, D. Zanchet, F.B. Noronha, J.M.C. Bueno, Appl. Catal. A 327 (2007) 197.
[16] M.C. Sanchez-Sanchez, R.M. Navarro, J.L.G. Fierro, Int. J. Hydrogen Energ. 32 (2007) 1471.
[17] A.J. Vizcaino, A. Carrero, J.A. Calles, Int. J. Hydrogen Energ. 32 (2007) 1461.
[18] M.N. Barroso, M.F. Gomez, L.A. Arrua, M.C. Abello, Appl. Catal. A 304 (2006) 116.
[19] F. Frusteri, S. Freni, V. Chiodo, S. Donato, G. Bonura, S. Cavallaro, Int. J. Hydrogen Energ. 31 (2006) 2193.
[20] H.V. Fajardo, L.F.D. Probst, Appl. Catal. A 306 (2006) 134.
[21] Y. Yang, J. Ma, F. Wu, Int. J. Hydrogen Energ. 31 (2006) 877.
[22] M.H. Youn, J.G. Seo, P. Kim, J.J. Kim, H.-I. Lee, I.K. Song, J. Power Sources 162 (2006) 1270.
[23] B. Zhang, X. Tang, Y. Li, W. Cai, Y. Xu, W. Shen, Catal. Commun. 7 (2006) 367.
[24] A.J. Akande, R.O. Idem, A.K. Dalai, Appl. Catal. A 287 (2005) 159.
[25] J. Kugai, S. Velu, Ch. Song, Catal. Lett. 101 (2005) 255.
[26] J. Sun, X.-P. Qiu, F. Wu, W.-T. Zhu, Int. J. Hydrogen Energ. 30 (2005) 437.
[27] S. Velu, K. Suzuki, M. Vijayaraj, S. Barman, Ch.S. Gopinath, Appl. Catal. B 55 (2005) 287.
[28] J. Comas, F. Marino, M. Laborde, N. Amadeo, Chem. Eng. J. 98 (2004) 61.
[29] F. Frusteri, S. Freni, L. Spadaro, V. Chiodo, G. Bonura, S. Donato, S. Cavallaro, Catal. Commun. 5 (2004) 611.
[30] F. Frusteri, S. Freni, V. Chiodo, L. Spadaro, O. Di Blasi, G. Bonura, S. Cavallaro, Appl. Catal. A: Gen. 270 (2004) 1.
[31] F. Frusteri, S. Freni, V. Chiodo, L. Spadaro, G. Bonura, S. Cavallaro, J. Power Sources 132 (2004) 139.
[32] A.N. Fatsikostas, X.E. Verykios, J. Catal. 225 (2004) 439.
[33] F. Marino, M. Boveri, G. Baronetti, M. Laborde, Int. J. Hydrogen Energ. 29 (2004) 67.
[34] J. Sun, X. Qiu, F. Wu, W. Zhu, W. Wang, S. Hao, Int. J. Hydrogen Energ. 29 (2004) 1075.
[35] S. Freni, S. Cavallaro, N. Mondello, L. Spadaro, F. Frusteri, Catal. Commun. 4 (2003) 259.
[36] F. Marino, G. Baronetti, M. Jobbagy, M. Laborde, Appl. Catal. A 238 (2003) 41.
[37] D. Srinivas, C.V.V. Satyanarayana, H.S. Potdar, P. Ratnasamy, Appl. Catal. A 246 (2003) 323.
[38] A.N. Fatsikostas, D.I. Kondarides, X.E. Verykios, Catal. Today 75 (2002) 145.
[39] S. Freni, S. Cavallaro, N. Mondello, L. Spadaro, F. Frusteri, J. Power Sources 108 (2002) 53.
[40] S. Velu, N. Satoh, Ch.S. Gopinath, K. Suzuki, Catal. Lett. 82 (2002) 145.
[41] A.N. Fatsikostas, D.I. Kondarides, X.E. Verykios, Chem. Commun. (2001) 851.
[42] F. Marino, M. Boveri, G. Baronetti, M. Laborde, Int. J. Hydrogen Energ. 26 (2001) 665.
[43] F.J. Marino, E.G. Cerrella, S. Duhalde, M. Jobragy, M.A. Laborde, Int. J. Hydrogen Energ. 23 (1998) 1095.
[44] E.B. Barrett, L.G. Joyner, P.P. Halenda, J. Am. Chem. Soc. 73 (1951) 373.
[45] N.M. Markovic, P.N. Ross, CATTECH 4 (2000) 110.